Energy Proceedings
Vol 54, 2025
ISSN 2004-2965

A comparative numerical study on heat transfer analysis between single-channel-type large diameter heat exchanger with that of multi-channel-type small hydraulic diameter heat exchanger using Super-critical CO_2[#]

Samir Nanda[1*], Sourav Mitra[1]

1 Department of Mechanical Engineering, Indian Institute of Technology Kharagpur

Kharagpur- 721302, West Bengal, India

(Corresponding Author: samir.nanda@kgpian.iitkgp.ac.in)

ABSTRACT

The supercritical carbon dioxide (s-CO_2) Brayton cycle is one of the recommended power cycles for next generation high efficiency power plants. An additional benefit of using this working fluid is the miniaturised moving parts when compared to conventional Rankine or Brayton cycle. However, one of the challenges is the miniaturised design of heat exchangers used in gas cooler, gas heater and regenerators. This can be achieved by reducing the hydraulic diameter of fluid flow channel. However, heat transfer coefficients for supercritical CO_2 flow through such miniaturised channels are yet to be studied. In any heat exchanger, the decrease in hydraulic diameter of the channel leads to a higher heat transfer coefficient at the expense of higher pumping power. This study deals with the comparison of a large-diameter single-channel type (SCT) heat exchanger and a small hydraulic diameter multi-channel type (MCT) heat exchanger using s-CO_2. A numerical investigation is done on a tube-in-tube type heat exchanger, and the effect of mass flow rate and channel diameter at the given inlet temperature and pressure is depicted. At 3 different mass flow rates, such as 1 kg/hr, 3 kg/hr, and 4 kg/hr, the percentage enhancement in the rate of heat transfer for MCT is found to be higher w.r.t. SCT, by 33.4%, 30.34%, and 25%, respectively.

Keywords: Brayton cycle, Heat Exchanger, Super-critical CO_2

NONMENCLATURE

Abbreviations	
MCT	Multi-channel type
SCT	Single-channel type
s-CO_2	Super-critical carbon dioxide
Symbols	
A_c	Cross-sectional area [m^2]
A_s	Heat transfer surface area [m^2]
D_h	Hydraulic diameter [m]
h	Heat transfer coefficient [W/m^{2}K]
i	Enthalpy [J/kg]
L	Length [m]
$\dot{m}$	Mass flow rate [kg/s]
P	Wetted perimeter [m]
T	Temperature [K]
Subscripts	
b	Bulk
in	Inlet
out	Outlet
wi	Inner wall

1. INTRODUCTION

Carbon dioxide is one of the commonly used supercritical fluids that has gained significant attention over the past few years. This fluid's stability, low cost, non-flammability, non-toxicity, and reliability created tough competition for other working fluids in trans-critical cycles. Its abundance in nature makes it easy to

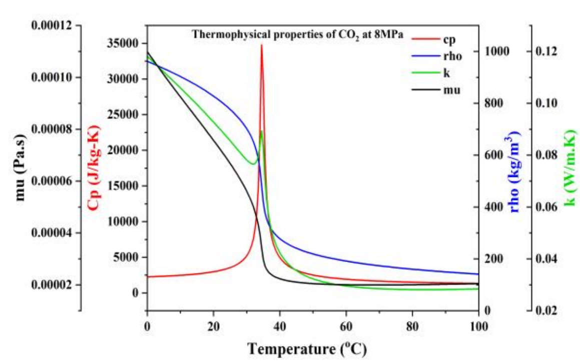

Fig. 1 Property plot for s-CO_2 for 8 MPa

This is a paper for the 16th International Conference on Applied Energy (ICAE2024), Sep. 1-5, 2024, Niigata, Japan.

obtain. CO_2 attains a supercritical state when it is above its critical temperature (31.2°C) and critical pressure (7.39 MPa). The fact that conventional refrigerants have negative impacts on CFCs and HCFCs in the atmosphere, leading to ozone layer depletion and global warming, makes the urgency of replacing such refrigerants a global concern. The ozone layer depletion (ODP) and global warming potential (GWP) of CO_2 are 0 and 1, respectively, making it more environmentally friendly compared to other refrigerants. One of the recommended power cycles for use is the supercritical carbon dioxide (s-CO_2) Brayton cycle, which maintains a single phase throughout the cycle, thereby simplifying plant design. A CO_2-based Brayton cycle can result in higher thermal efficiency when working at high temperatures. CO_2 exhibits unique thermophysical properties in the supercritical state, where it behaves neither like a gas nor a liquid. The s-CO_2 Brayton cycles take advantage of these properties, such as high density, low viscosity, and high heat transfer rates, to achieve higher efficiencies. Due to the dramatic behaviour of the specific heat capacity of CO_2 at the pseudo-critical region, as shown in figure (1), the local heat transfer coefficient gets enhanced in that region, thus helping in creating effective gas coolers/condensers.

Previously, many authors had worked on single channel-based heat exchangers using s-CO_2 and determined the effect of channel geometry, thermophysical properties, operating pressure range, inlet bulk temperature, and mass flux on heat transfer characteristics. Liao, Zhao, et al. (2002) did an experiment on six stainless steel circular tubes having internal diameters of 0.50 mm, 0.70 mm, 1.10 mm, 1.40 mm, 1.55 mm, and 2.16 mm respectively, were cooled to a constant temperature. They tested these tubes at temperatures ranging from 20 to 110 °C and carbon dioxide pressures ranging from 74 to 120 bar, developing a new correlation for the axially averaged Nusselt number [1]. Dang, Chaobin, et al. (2004) conducted an experimental study on the heat transfer coefficient and pressure drop for various cooling tube diameters, ranging from 1 mm to 6 mm and their experimental results were 20% more accurate than known correlations [2]. Similarly, other authors have reported single-channel horizontally orientated heat exchangers and analysed their heat transfer characteristics as well [3], [4], [5]. There are some studies on multi-channel heat exchangers in which decreasing the hydraulic diameter leads to an increase in heat transfer coefficient. This is achieved using compact heat exchangers such as PCHEs (printed circuit heat exchangers). A. Meshram et al. (2016) numerically performed for straight and zig-zag channels in fully turbulent conditions and found that a larger bend angle and smaller linear pitch perform better than a smaller bend angle and large linear pitch combination [6].

It is evident from the literature that many authors have done analysis on single channels, which are easily fabricated, and then moved on to small hydraulic-diameter multi-channels, i.e., PCHEs, which are fabricated using chemical etching and diffusion bonding processes. Given the fact that there is scarcity of research on comparing the heat transfer characteristics of single-channel and multi-channel heat exchangers,

Single-Channel-Type			**Multi-Channel-Type**	
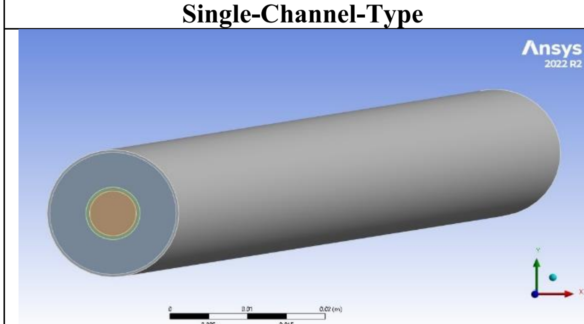			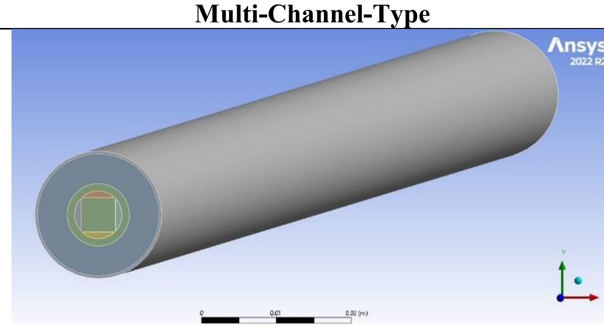	
Outer tube: **OD:** 17 mm **ID:** 16.35 mm	**Inner tube:** **OD:** 7 mm **ID:** 6.35 mm **D_h for CO_2 side** = 6.35 mm		**Outer tube:** **OD:** 17 mm **ID:** 16.35 mm	**Inner tube:** **OD:** 8.35 mm **ID:** 6.35 mm **Square rod length:** 4.6 mm **D_h for CO_2 side** = 1.2 mm
Length of the test section: 750 mm				

Fig. 2 Geometry Details of the heat exchangers

this paper aims to present a comparative study between these two configurations. Also, as the hydraulic diameter decreases, the heat transfer coefficient increases. However, the effect on the net heat transfer enhancement due to the small hydraulic diameter and multiple channels needs to be determined.

2. GEOMETRY DETAILS AND NUMERICAL MODEL

2.1 Geometrical Model

In a counterflow heat exchanger mechanism, the comparative numerical study on heat transfer analysis between large-diameter single-channel and small hydraulic-diameter multi-channel heat exchangers was conducted. A single channel type (SCT), which is a concentric tube-in-tube type heat exchanger. The SCT consists of an outer tube with ID 16.35 mm and OD 17 mm and an inner tube with ID 6.35 mm and OD 7 mm. The SCT heat exchanger is 750 mm in length. CO_2 flows through the inner tube, while water flows through the outer annulus. For a comparative study, a multi-channel type (MCT) is considered, which is also a concentric tube-in-tube heat exchanger having just a solid square rod of 4.6 mm edge length being inserted into the inner tube such that four semi-circular multiple channels are created within the single inner tube while other dimensions of the MCT have been kept the same as those of the SCT. The fabrication of this novel configuration of MCT is easy and does not require any advanced, expensive manufacturing techniques thus making it cost-effective.

2.2 Numerical Details

In the present study, based on the finite volume method (FVM), the commercial software ANSYS FLUENT 22 R2 was used to solve a 3-dimensional turbulent flow at steady state with no gravity involved. The flow and heat transfer processes satisfy the conservation equations, which include the continuity equation, momentum equation, energy equation, and additionally the turbulence model Shear Stress Transport (SST) $k-\omega$ to capture the near-wall behavior in the fluid flow.

The equation of state for super-critical CO_2 (s-CO_2) was obtained from the standard reference database NIST (REFPROP) Version 9.0, integrated directly from the Fluent Material Property Section (real-gas-nist). The properties of liquid water and steel were considered constant and obtained directly from the Fluent database.

We set the inlet as the mass-flow-inlet and the outlet as the pressure-outlet. The fluid and solid boundaries were set as coupled, no-slip walls. The pressure and velocity were coupled by the SIMPLEC algorithm, and the energy equations and turbulent parameters adopted the Second-Order-Upwind scheme. The simulation was regarded as converged when the residual errors for continuity, momentum, and $k-\omega$ equations were less than 10^{-4} and the convergence residuals of the energy equation were less than 10^{-7}.

2.3 Governing Equations

The governing equations for conservation of mass, momentum and energy are as follows:

Continuity Equation:

$$\frac{\partial(\rho u_i)}{\partial x_i}=0 \tag{1}$$

Momentum Equation:

$$\frac{\partial(\rho u_i u_j)}{\partial x_j}=-\frac{\partial p}{\partial x_i}+\frac{\partial}{\partial x_j}\left[\mu_{eff}\left(\frac{\partial u_i}{\partial x_j}+\frac{\partial u_j}{\partial x_i}\right)-\frac{2}{3}\mu_{eff}\frac{\partial u_k}{\partial x_k}\right] \tag{2}$$

Energy Equation:

$$\frac{\partial}{\partial x_i}\left(\rho u_i c_p T\right)=\frac{\partial}{\partial x_i}\left[\lambda\frac{\partial T}{\partial x_i}\right] \tag{3}$$

$$\frac{\partial}{\partial x_i}\left(\lambda_s\frac{\partial T}{\partial x_j}\right)=0 \tag{4}$$

Where ρ , c_p and λ respectively denote the density, specific heat at constant pressure and thermal conductivity; p and T are the pressure, temperature, respectively; μ_{eff} is the effective turbulent viscosity and equals to the sum of dynamic viscosity μ and turbulent viscosity μ_t ; u and x respectively represent the velocity and coordinate axis; and subscripts i, j and k respectively are the components of the coordinates.

The SST $k-\omega$ turbulent model has been adopted for s-CO_2 heat transfer numerical simulation [7].

Turbulent Kinetic Energy (k) Equation:

$$\frac{\partial}{\partial x_j}\left(\rho k u_i\right)=\frac{\partial}{\partial x_j}\left(\Gamma_k\frac{\partial k}{\partial x_j}\right)+G_k-Y_k \tag{5}$$

Turbulent Specific Dissipation Rate (ω) Equation:

$$\frac{\partial}{\partial x_j}\left(\rho\omega u_i\right)=\frac{\partial}{\partial x_j}\left(\Gamma_\omega\frac{\partial\omega}{\partial x_j}\right)+G_\omega-Y_\omega+D_\omega \tag{6}$$

Where G_k and G_ω respectively denote the generation term of k and ω; Γ_k and Γ_ω respectively denote effective diffusivity of k and ω; Y_k and Y_ω respectively denote the dissipation of k and ω due to turbulence; and D_ω is the cross-diffusion term.

2.4 Data Reduction

The rate of heat transfer is calculated using the following expression;

$$q = \dot{m}(i_{in} - i_{out}) \tag{7}$$

The hydraulic diameter can be found from the following expression;

$$D_h = \frac{4A_c}{P} \tag{8}$$

The bulk temperature is evaluated using;

$$T_b = \frac{T_{in} - T_{out}}{2} \tag{9}$$

The local convective heat transfer coefficient along the flow direction is calculated using the Newton's law of cooling;

$$h = \frac{q}{A_s(T_b - T_{w,i})} \tag{10}$$

$$A_s = \pi D_h L \tag{11}$$

2.5 Grid independence Test

The grid independence test included the discretization of solid and fluid domains using ANSYS workbench meshing. For different set of mesh elements, the variation of average heat transfer coefficient is observed. The minimum number of elements for SCT was chosen to be 15.02 lakhs and 36.47 lakhs for MCT for a constant average heat transfer coefficient.

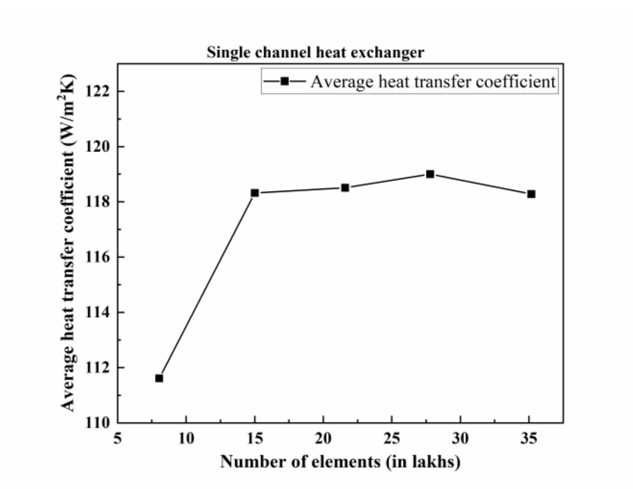

Fig. 3 Grid independence test for SCT heat exchanger

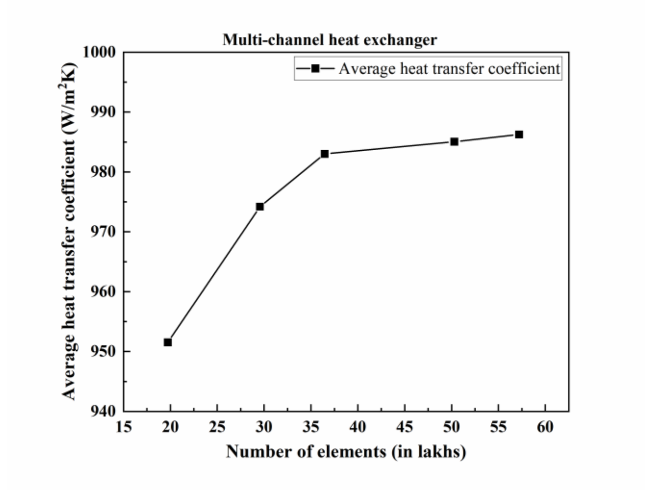

Fig. 4 Grid independence test for MCT heat exchanger

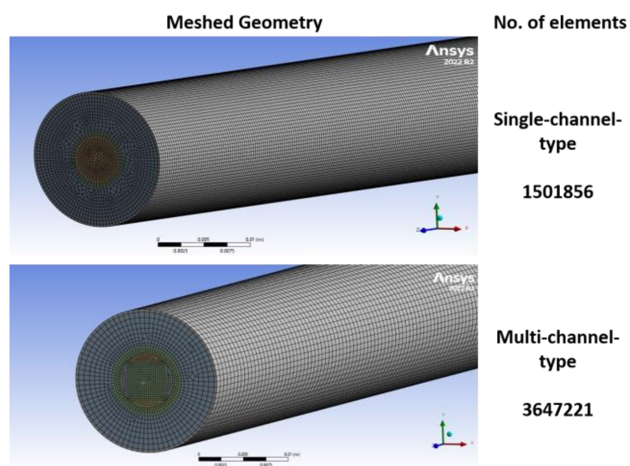

Fig. 5 Meshed model

2.6 Validation of Numerical Model

As shown in Ref. [2], at steady state, the test conditions are as follows: diameter of the tube is 6 mm, operating pressure as 8 MPa, heat flux being 12 kW/m^2, mass flux of 200 kg/m^2-s (m = 0.005652 kg/s) and inlet temperatures varied from 30 - 70°C. Figure (4) shows the numerical results based on SST $k-\omega$ turbulence model which has been validated and shows agreement is well with the experimental data from Dang et al.[2]. The y-coordinate is the average heat transfer coefficient which is calculated as the ratio of heat flux and temperature difference between meal bulk temperature of CO_2 and the inner wall. The mean bulk temperature is the average of the inlet and outlet temperature of the test section.

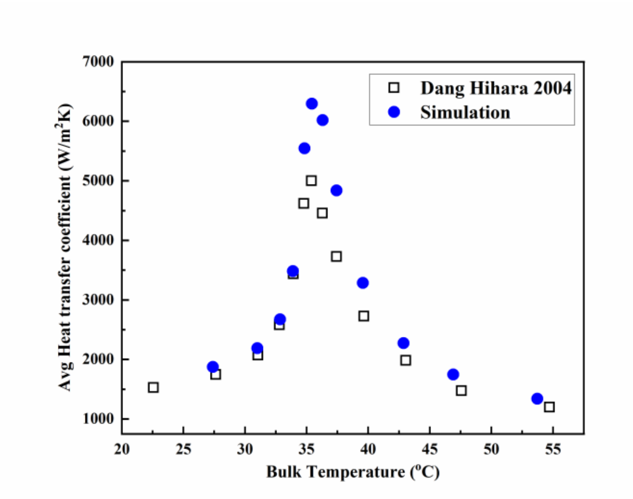

Fig. 6 Numerical model validation for bulk variation of temperature and average heat transfer coefficient

3. RESULTS AND DISCUSSION

3.1 Effect of mass flow rate

3.1.1 Heat transfer coefficient

Figure (7 & 8) shows the local variation of the heat transfer coefficient from the CO_2 side at different mass flow rates in the case of SCT and MCT heat exchangers. The local heat transfer coefficient decreases initially in the developing region of flow as the boundary layer thickness increases. In the mid-section, the variation is mostly constant. On approaching the end of the flow, as it reaches and attains the pseudo-critical temperature, the specific heat capacity at constant pressure spikes. Due to this reason, the local heat transfer coefficient at 1 kg/hr seems to be increasing towards the end of the flow, as seen from figures (7,8). Furthermore, as the mass flow rate increases, the temperature approaches the pseudo-critical temperature but doesn't quite attain it. Although the local heat transfer coefficient increases with an increase in mass flow rates, there is not much variation at the mid-section and towards the end of the channel in cases of 3 kg/hr and 4 kg/hr. It is also observed that in the case of SCT, the local heat transfer coefficient is significantly lower than that of MCT. This is because the hydraulic diameter of MCT is lower than that of SCT, i.e., 1.2 mm and 6.35 mm, respectively. With the decrease in diameter, the heat transfer coefficient increases; however, this analogy is not enough to convey MCT's performance better than that of SCT. The net rate of heat transfer can confirm more about the performances.

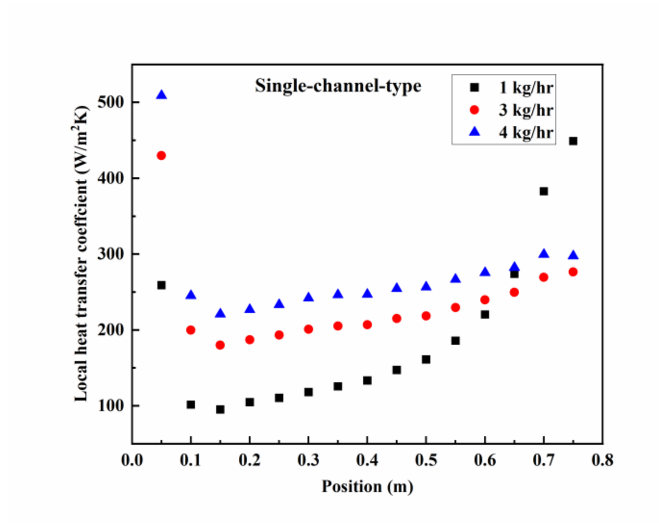

Fig. 7 CO_2 side local heat transfer coefficient at different mass flow rates for SCT heat exchangers where CO_2 inlet temperature is 368K and pressure 8 MPa and water inlet temperature is 283K at 1 kg/hr

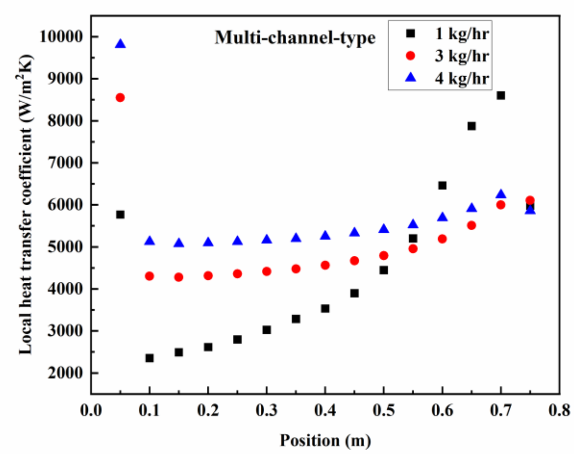

Fig. 8 CO_2 side local heat transfer coefficient at different mass flow rates for MCT heat exchangers where CO_2 inlet temperature is 368K and pressure 8 MPa and water inlet temperature is 283K at 1 kg/hr

3.1.2 Net heat transfer

Figure (9) illustrates the net variation of the rate of heat transfer at different mass flow rates for SCT and MCT heat exchangers. The rate of heat transfer increases with mass flow rates. The net rate of heat transfer is higher in the case of MCT compared to SCT, as seen in figure (9). This is due to the fact that the change in enthalpy along the length is greater in MCT than in SCT.

Therefore, an enhancement in the rate of heat transfer is observed in figure (9). It is also observed that at low mass flow rates such as 1 kg/hr, the percentage enhancement is higher, i.e., 33.4%, compared to higher mass flow rates, i.e., 30.34% and 25% for 3 kg/hr and 4 kg/hr, respectively. Hence, with the increase in mass flow rates, the percentage enhancement decreases, which conveys that the rate of heat transfer would tend to have similar values for both channel types at higher flow rates.

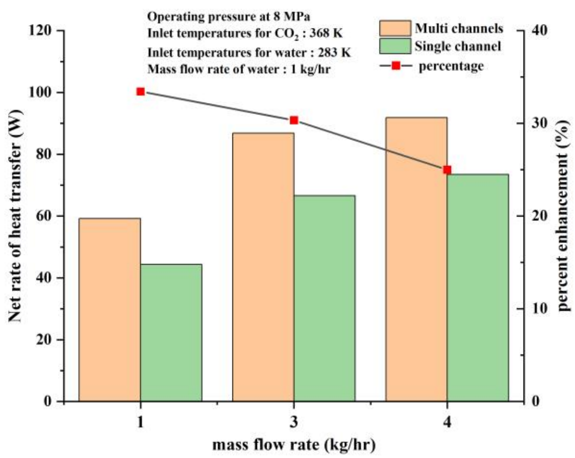

Fig. 9 Net variation of rate of heat transfer at different mass flow rates for SCT and MCT heat exchangers

3.1.3 Pressure Drop

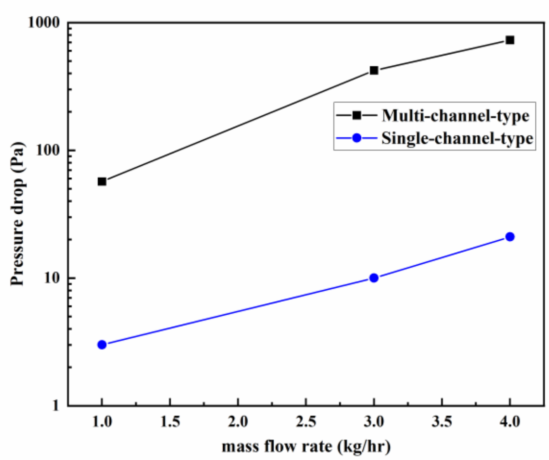

Fig. 10 Pressure drop across the channel at different mass flow rates for SCT and MCT heat exchangers where CO_2 inlet temperature is 368K and pressure 8 MPa and water inlet temperature is 283K at 1 kg/hr

Figure (10) illustrates the change in pressure drop across the entire length of the channel at various mass flow rates for SCT and MCT heat exchangers. In the case of SCT, the hydraulic diameter is greater than that of MCT, resulting in a lower pressure drop. Despite having significant pressure drop in the case of MCT, when the line pressure is 8 MPa, a drop-in pressure of approximately 700 Pa is actually quite minimal. This trade-off is essential to maintain the enhancement in the rate of heat transfer. The lower-pressure drop value is the result of CO_2's unique thermophysical property feature, i.e., its dynamic viscosity, whose magnitude is very less, by the order of 10^{-4}, in the pseudo-critical region.

4. CONCLUSION

For the comparative numerical study on heat transfer analysis of the SCT and MCT heat exchangers with varying mass flow rates, the following conclusions were drawn;

- The local heat transfer coefficient increases with an increase in mass flow rates. With the decrease in hydraulic diameter of the channel from SCT to MCT, the local heat transfer coefficient in the case of MCT is significantly higher compared to the SCT heat exchanger. MCT attains a pseudo-critical region towards the end of the channel, which largely influences the increment in heat transfer coefficient.
- At low mass flow rates such as 1 kg/hr, the percentage enhancement in the net rate of heat transfer for MCT is higher w.r.t. SCT, i.e., 33.4%, compared to higher mass flow rates, i.e., 30.34% and 25% for 3 kg/hr and 4 kg/hr, respectively. However, the pressure drop in MCT is larger compared to SCT which is an essential trade off keeping the enhancement of heat transfer in mind.

ACKNOWLEDGEMENT

The work presented in this paper is supported by the grant from Department of Science and Technology (DST), Government of India (Grant no.: TMD/CERI/CleanCoal/2017/034 (IIT KGP) (G)).

The author acknowledges the funding received from IIT Kharagpur to attend the conference.

REFERENCE

[1] S. M. Liao and T. S. Zhao, “Measurements of heat transfer coefficients from supercritical carbon dioxide flowing in horizontal mini/micro

channels," *J Heat Transfer*, vol. 124, no. 3, pp. 413–420, Jun. 2002, doi: 10.1115/1.1423906.

[2] C. Dang and E. Hihara, "In-tube cooling heat transfer of supercritical carbon dioxide. Part 1. Experimental measurement," in *International Journal of Refrigeration*, Elsevier Ltd, 2004, pp. 736–747. doi: 10.1016/j.ijrefrig.2004.04.018.

[3] S. H. Yoon, J. H. Kim, Y. W. Hwang, M. S. Kim, K. Min, and Y. Kim, "Heat transfer and pressure drop characteristics during the in-tube cooling process of carbon dioxide in the supercritical region," *International Journal of Refrigeration*, vol. 26, no. 8, pp. 857–864, Dec. 2003, doi: 10.1016/S0140-7007(03)00096-3.

[4] S. S. Pitla, E. A. Groll, and S. Ramadhyani, "New correlation to predict the heat transfer coefficient during in-tube cooling of turbulent supercritical CO 2." [Online]. Available: www.elsevier.com/locate/ijrefrig

[5] C. H. Son and S. J. Park, "An experimental study on heat transfer and pressure drop characteristics of carbon dioxide during gas cooling process in a horizontal tube," *International Journal of Refrigeration*, vol. 29, no. 4, pp. 539–546, Jun. 2006, doi: 10.1016/j.ijrefrig.2005.10.010.

[6] A. Meshram *et al.*, "Modeling and analysis of a printed circuit heat exchanger for supercritical CO2 power cycle applications," *Appl Therm Eng*, vol. 109, pp. 861–870, Oct. 2016, doi: 10.1016/j.applthermaleng.2016.05.033.

[7] H. Pu *et al.*, "Numerical investigation on turbulent mixed convective heat transfer of CO2 in a horizontal miniature tube at supercritical pressure," *International Journal of Thermal Sciences*, vol. 184, Feb. 2023, doi: 10.1016/j.ijthermalsci.2022.107992.